STUDY OF THE ^{22}Ne$(p,\gamma)^{23}$Na REACTION AT LUNA*

A. Caciolli

on behalf of the LUNA Collaboration

University and INFN of Padua, Padua, Italy

(Received January 7, 2020)

The ^{22}Ne$(p,\gamma)^{23}$Na reaction, part of the neon–sodium cycle of hydrogen burning, may explain the observed anticorrelation between sodium and oxygen abundances in globular cluster stars. At the astrophysical energies, the presence of many resonances dominates the rate. The LUNA Collaboration measured for the first time three of them: $E_p = 156.2$, 189.5, and 259.7 keV. Recently, by using a high-efficiency setup, the uncertainties related to those three states have been lowered drastically and the direct component of the cross section was also measured. As a result, at a temperature of 0.1 GK, the error bar of the ^{22}Ne$(p,\gamma)^{23}$Na reaction rate is now reduced by three orders of magnitude. The new high-efficiency setup provides also a possibility to investigate the branching cascades, despite the limited resolution of the BGO detector.

DOI:10.5506/APhysPolB.51.641

1. Introduction

Hydrogen burning proceeds through several phases and there are many cycles converting protons in helium by means of proton-induced reactions on heavier elements. The neon–sodium cycle proceeds in advanced stages of hydrogen burning and it is critical for the synthesis of the neon or sodium isotopes, but also that of magnesium or aluminum. In particular, the NeNa cycle contributes in a negligible way to the energy budget of stars, but it affects the abundances of the elements between ^{20}Ne and ^{27}Al [1].

An anticorrelation of sodium and oxygen abundances has been observed in red giant stars of globular clusters [2]. The material involved in the anticorrelation can be produced in hydrogen burning when the temperature is high enough to ignite not only the CNO cycle, but also the NeNa one [3].

* Presented at the XXXVI Mazurian Lakes Conference on Physics, Piaski, Poland, September 1–7, 2019.

Possible explanations of this effect should involve the mechanism which describes the formation of pollution of the interstellar medium due to the ashes from previous generation stars. For this, several candidates have been discussed and proposed: intermediate-mass asymptotic giant branch (AGB) stars or super AGB stars [4–6], fast rotating massive stars [7], supermassive stars [8], massive stars in close binary systems [9], stellar collisions [10], and classical novae [11]. The thermonuclear reaction cross sections, participating in the CNO and the NeNa cycles, clearly need to be well-understood. The latter one is composed of several reactions as depicted in Fig. 1. Among them, the slowest reaction rate is the one of the ^{20}Ne$(p,\gamma)^{21}$Na reaction, but before the study at LUNA [12], the ^{22}Ne$(p,\gamma)^{23}$Na was the reaction with the highest uncertainty of the entire cycle. This was mostly due to the presence of several resonances at stellar energies [13], where only upper limits were given in literature and, in particular, two databases reported a difference on the thermonuclear reaction rate of about a factor of 1000 [14, 15]. For this reason, a complete study of this reaction was initiated by the LUNA Collaboration [16]. This study was divided into two phases: one using a setup consisting of two high-purity germanium detectors, and the second one employing a high-efficiency 4π BGO detector.

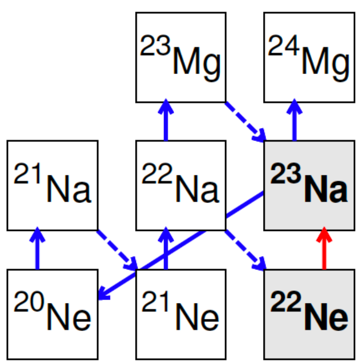

Fig. 1. (Color online) Scheme of the NeNa cycle. The solid arrows represent the various (p,γ) and (p,α) reactions involved in the cycle, while the β^+ decays are represented by dashed arrows. In gray/red, with shaded isotopes, the ^{22}Ne$(p,\gamma)^{23}$Na reaction is shown.

2. Fully shielded HPGe setup (Phase I)

^{23}Na has a quite complex level scheme and all the possible resonances are expected to decay through a complex branching cascade with γ rays in an energy range from 440 keV up to almost 8 MeV, due to the high Q-value of the ^{22}Ne$(p,\gamma)^{23}$Na reaction. In this context, the possibility to explore the different branching cascades by using a high resolution detector system was implemented at LUNA. The setup, consisting of two HPGe detectors [17], was installed on the beam-line dedicated for gas target experiments [18].

The position of LUNA under the Gran Sasso mountain provides a high reduction of the cosmic rays flux [19, 20], which guarantees 5 orders of magnitude reduction of the natural background for γ rays of energy above 3 MeV. In order to reduce the background also at lower energies, a shielding of few cm of copper and around 25 cm of lead is needed [21]. A reduction of the experimental background has also been observed for particle detectors in an underground environment [22, 23].

Thanks to two internal collimators, the detectors were looking at the gas in the chamber from an angle of 55° and 90°, respectively [17], in order to take into account possible effects due to the angular distribution of the emitted γ rays.

Using this setup, three resonances were observed directly for the first time [24–26] together with their branching cascades [27]. These resonances, at 156.2, 189.5, and 259.7 keV, were also observed by another experiment performed at the Triangle Universities Nuclear Laboratory (TUNL) with a solid target setup [28]. Recently, two other papers [29, 30] have been published, reporting results similar to those obtained by LUNA.

3. 4π-BGO setup (Phase II)

The HPGe phase was not able to investigate the direct capture component of the cross section due to the limited efficiency of the setup. In addition, there were still two debated resonances at 105 and 71 keV, where only upper limits were present in literature [15]. Those resonances were not included in the reaction rate calculation performed by the TUNL group at all [14]. With the HPGe phase, the upper limits on these two resonances were reduced and a new updated thermonuclear reaction rate was given and its astrophysical impact discussed [32], but they still remain a not negligible source of uncertainty for the nucleosynthesis calculations.

Therefore, we moved to a setup involving a high-efficiency detector. A new scattering chamber was installed on the same windowless gas target system used in the previous phase and surrounded with a 4π-BGO detector [33] covering almost the total solid angle. This way, the total efficiency was increased by a factor of 100 reaching a value of about 50%. The BGO detector is composed of six sectors each coupled with a PMT tube and acquired by a CAEN digitizer V1724 after a preamplifier. Each channel was acquired independently and then an add-back spectrum was created by summing all γ rays deposited in the detector in a time window of 350 μs. This way, the detector was used as a single crystal. A detailed discussion about the data acquisition can be found also in Refs. [33, 34]. The detection efficiency was checked by using two different simulation codes, one based on Geant3 [35] and one based on Geant4 [33], and constrained with experimental measurements performed with calibrated radioactive sources of ^{137}Cs, ^{60}Co, and ^{88}Y and the well-known $E_p = 278$ keV resonance of the $^{14}N(p,\gamma)^{15}O$ reaction [36, 37]. The high intensity proton beam of the LUNA-400kV accelerator [38] (around 200 μA) was stopped by a calorimeter, which determines the beam current by measuring the power, $W_{\rm beam}$, deposited by the beam. This quantity is related to the beam current (as the number of protons N_p) by the equation

$$N_p = \frac{W_{\rm beam}}{E_{\rm Cal}}\,, \tag{1}$$

where $E_{\rm Cal}$ is the beam energy on the calorimeter surface.

Even if the background in the LUNA environment is extremely suppressed, the beam-induced background is still present: boron [39], carbon, and fluorine [40] are the most problematic contaminants, since they have high cross sections for producing γ rays in proton-induced reactions at beam energies below 400 keV. In some cases, the beam induced background could come from the target itself [41–43]. For each beam energy used in the analysis, a long run with argon gas in the target chamber was acquired. Argon at the LUNA-400 energies is inert for γ-ray production via interaction with protons, therefore, it is ideal for such contaminant studies. In order to take into account the different energy loss of protons in neon and argon, the argon pressure was set in order to have the same energy loss in the target chamber as in the neon case. The most important source of beam-induced background during the experiment was due to the $^{11}B(p,\gamma)^{12}C$ reaction. Considering its high Q-value around 16 MeV, this reaction produces three peaks in the γ-ray spectrum at 16 MeV, 11 MeV, and 4.4 MeV corresponding to the transition to the ground state, the transition to the first excited state of ^{12}C, and its subsequent decay, respectively. In addition to this, a summing effect that enhances the 16-MeV peak is also present in the case of a setup like the one used in the present experiment. Despite the efforts of reducing the boron content in our setup surfaces, a residual quantity was unavoidable (at the level of several ppm, but still observable in the reduced environmental background of the National Laboratories of Gran Sasso). As those peaks cover a broad energy range, they were also used for energy calibration of the γ-ray spectra. Since in the runs with argon only the signal produced by the contaminants was present, they have been used to subtract this effect from the spectra with neon. It is evidenced by Fig. 2. A normalisation region was selected to cover properly the signal from the two high energy peaks from the $^{11}B(p,\gamma)^{12}C$ reaction. This region is shown in Fig. 2.

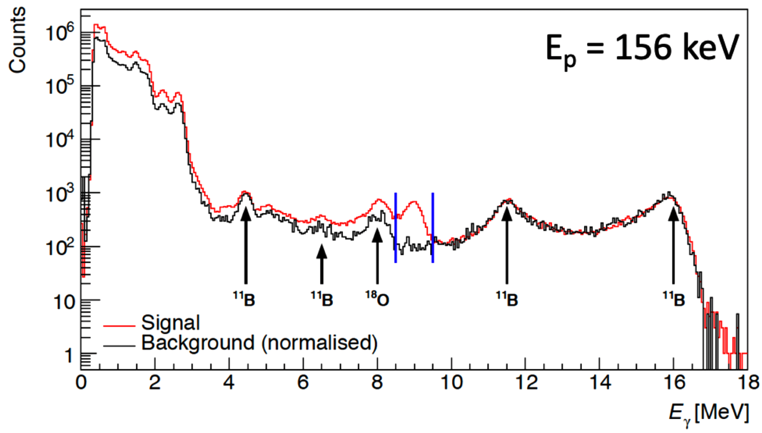

Fig. 2. (Color online) The experimental spectrum for the 156 keV resonance acquired using neon (argon) gas in gray/red (black). The two spectra are normalized to match the region E_γ = 10.5–17.0 MeV. The main sources of beam-induced background are also labeled in the figure.

Updated results for all the three previously observed resonances have been obtained in good agreement with the previous LUNA result [44]. In addition, for the two "supposed" low-energy resonances, at 70 and 105 keV, new upper limits, improved by a factor of 100, were provided leading to a negligible contribution of these two resonances in the astrophysical scenarios. In addition, for the first time, four points of the non-resonant component of the cross section were measured in the energy range from 310 keV down to below 200 keV. Those points provided a better constraint of the direct capture component of this reaction, as discussed in Ref. [44].

As discussed above, the add-back spectrum is obtained by an offline analysis that sums all γ rays observed by the whole detector in a defined time window. Reversing this procedure, we can gate on a selected region of the add-back spectrum and reconstruct the single spectra corresponding only to the events in the region selected in the add-back spectrum. Using this approach, the branching cascades of one of the three resonances, at 189 keV, were obtained [33], while for all other resonances and the direct capture component, the analysis is still ongoing. Despite the poor resolution of the BGO detector, we were able to observe all cascades transitions as shown in Fig. 3. In particular, the figure confirms that this analysis is sensitive to a possible transition to the ground state as claimed by Ref. [28], which was not observed in our spectra. This is a powerful use of this detector that will be applied soon to the other resonances and to the direct capture runs. In this latter case, the poor statistics increase the uncertainties related to the fitting procedure due to the less defined shape of some peaks. Therefore, the evaluation of this contribution to the uncertainty is still under study.

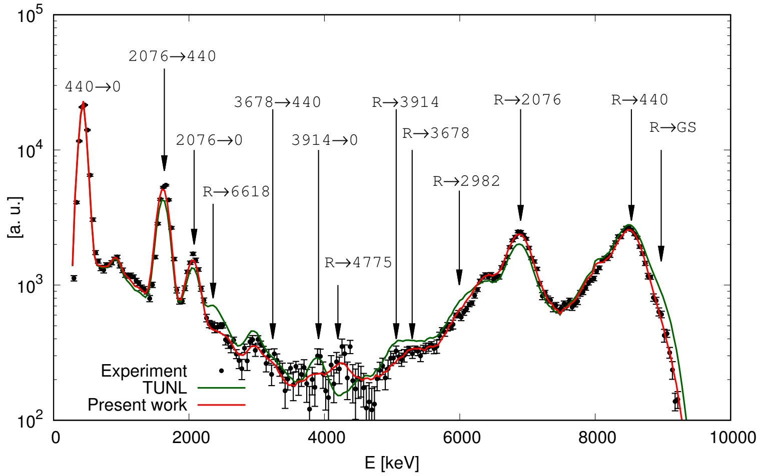

Fig. 3. Single sum spectrum on top of the 189.5 keV resonance in ^{22}Ne$(p,\gamma)^{23}$Na, gated on the add-back energy in the sum peak, $E^{\gamma}_{\rm sum}$ [8.0;9.7] MeV. The data are compared with simulated branchings from TUNL [28] and the best fit results from the present data, LUNA-BGO.

4. Conclusion

The LUNA Collaboration has studied the ^{22}Ne$(p,\gamma)^{23}$Na reaction in two distinct experimental campaigns. In the first one, a high-resolution detection system with two fully shielded high-purity germanium detectors was used, while the second phase employed a high-efficiency 4π-BGO setup. Thanks to this study, three resonances at 156, 189 and 260 keV were observed for the first time and the direct capture component of the cross section was determined for the first time below 300 keV in the center-of-mass frame. Thanks to these results, the new compiled thermonuclear reaction rate reports an overall uncertainty which is below the 10% — in perfect agreement with the request of stellar models.

REFERENCES

[1] J. Marion, W. Fowler, *Astrophys. J.* **125**, 221 (1957).

[2] R.G. Gratton, E. Carretta, A. Bragaglia, *Astron. Astrophys. Rev.* **20**, 50 (2012).

[3] N. Prantzos, C. Charbonnel, C. Iliadis, *Astron. Astrophys.* **470**, 179 (2007).

[4] P. Ventura, M. Di Criscienzo, R. Carini, F. D'Antona, *Mon. Not. R. Astron. Soc.* **431**, 3642 (2013).

[5] P. Ventura *et al.*, *Astrophys. J. Lett.* **761**, L30 (2012).

[6] C.L. Doherty *et al.*, *Mon. Not. R. Astron. Soc.* **437**, 195 (2014).

[7] T. Decressin *et al.*, *Astron. Astrophys.* **464**, 1029 (2007).
[8] P.A. Denissenkov *et al.*, *Mon. Not. R. Astron. Soc.* **448**, 3314 (2015).
[9] S.E. de Mink, O.R. Pols, N. Langer, R.G. Izzard, *Astron. Astrophys.* **507**, L1 (2009).
[10] A. Sills, E. Glebbeek, *Mon. Not. R. Astron. Soc.* **407**, 277 (2010).
[11] T.J. Maccarone, D.R. Zurek, *Mon. Not. R. Astron. Soc.* **423**, 2 (2012).
[12] A. Boeltzig *et al.*, *Eur. Phys. J. A* **52**, 75 (2016).
[13] R. Depalo *et al.*, *Phys. Rev. C* **92**, 045807 (2015).
[14] R. Longland *et al.*, *Nucl. Phys. A* **841**, 1 (2010).
[15] C. Angulo *et al.*, *Nucl. Phys. A* **656**, 3 (1999).
[16] C. Broggini, D. Bemmerer, A. Caciolli, D. Trezzi, *Prog. Part. Nucl. Phys.* **98**, 55 (2018).
[17] F. Cavanna *et al.*, *Eur. Phys. J. A* **50**, 179 (2014).
[18] A. Best *et al.*, *Eur. Phys. J. A* **52**, 72 (2016).
[19] D. Bemmerer *et al.*, *Eur. Phys. J. A* **24**, 313 (2005).
[20] T. Szücs *et al.*, *Eur. Phys. J. A* **44**, 513 (2010).
[21] A. Caciolli *et al.*, *Eur. Phys. J. A* **39**, 179 (2009).
[22] C.G. Bruno *et al.*, *Eur. Phys. J. A* **51**, 94 (2015).
[23] C.G. Bruno *et al.*, *Phys. Rev. Lett.* **117**, 142502 (2016).
[24] F. Cavanna *et al.*, *Phys. Rev. Lett.* **115**, 252501 (2015).
[25] F. Cavanna *et al.* [LUNA Collaboration], *Phys. Rev. Lett.* **120**, 239901 (2018).
[26] D. Bemmerer *et al.*, *Eur. Phys. Lett.* **122**, 52001 (2018).
[27] R. Depalo *et al.* [LUNA Collaboration], *Phys. Rev. C* **94**, 055804 (2016).
[28] K.J. Kelly *et al.*, *Phys. Rev. C* **95**, 015806 (2017).
[29] M. Williams *et al.*, arXiv:1910.01698 [nucl-ex].
[30] A. Lennarz *et al.*, arXiv:1910.00791 [nucl-ex].
[31] F. Cavanna, Ph.D. Thesis, Università degli studi di Genova, 2015.
[32] A. Slemer *et al.*, *Mon. Not. R. Astron. Soc.* **465**, 4817 (2017).
[33] F. Ferraro *et al.*, *Eur. Phys. J. A* **54**, 44 (2018).
[34] A. Boeltzig *et al.*, *J. Phys. G: Nucl. Part. Phys.* **45**, 025203 (2018).
[35] C. Casella *et al.*, *Nucl. Instrum. Methods Phys. Res. A* **489**, 160 (2002).
[36] M. Marta *et al.*, *Phys. Rev. C* **81**, 055807 (2010).
[37] M. Marta *et al.*, *Phys. Rev. C* **83**, 045804 (2011).
[38] A. Formicola *et al.*, *Nucl. Instrum. Methods Phys. Res. A* **507**, 609 (2003).
[39] D. Bemmerer *et al.*, *J. Phys. G: Nucl. Part. Phys.* **36**, 045202 (2009).
[40] A. Caciolli *et al.*, *Eur. Phys. J. A* **48**, 144 (2012).
[41] M. Anders *et al.*, *Eur. Phys. J. A* **49**, 28 (2013).
[42] M. Anders *et al.*, *Phys. Rev. Lett.* **113**, 042501 (2014).
[43] D. Trezzi *et al.*, *Astropart. Phys.* **89**, 57 (2017).
[44] F. Ferraro *et al.*, *Phys. Rev. Lett.* **121**, 172701 (2018).